Geophys. J. Int. (1994) **117**, 394–402

The magnetostrophic rise of a buoyant parcel in the Earth's core

H. K. Moffatt[1] and D. E. Loper[2]

[1]*Department of Applied Mathematics and Theoretical Physics, University of Cambridge, Silver Street, Cambridge* CB3 9EW, *UK*
[2]*Geophysical Fluid Dynamics Institute, Florida State University, Tallahassee, FL* 32306-3027, *USA*

Accepted 1993 September 21. Received 1993 September 21; in original form 1993 April 30

SUMMARY

The dynamics of a buoyant parcel (or blob) of fluid released from the mushy zone on the inner core boundary (ICB) is considered. Estimates of the density defect and of the rise velocity are obtained from consideration of mass conservation and magnetostrophic force balance. When Lorentz and Coriolis forces are of comparable orders of magnitude, the disturbance remains localized in a neighbourhood of the blob even in the absence of viscous effects, and an inviscid analysis is possible. The instantaneous velocity and magnetic field associated with a given localized buoyancy distribution are then determined, and on the assumption that the velocity is approximately uniform throughout the blob, its trajectory from ICB to core–mantle boundary (CMB) is deduced. Both westward drift and poleward migration of erupting field loops are indicated. The effects of turbulent diffusion on the blob are considered. The prospects for constructing a dynamo theory based on this 'blob scenario' are discussed.

Key words: compositional convection, core–mantle boundary, geodynamo, liquid core, magnetostrophic.

1 INTRODUCTION

It is now widely accepted that the Earth's magnetic field is powered by self-exciting dynamo action associated with fluid motion in the outer liquid core. The most plausible source of this motion is an instability of gravitational origin associated with the cooling of the Earth and the slow solidification of the inner core (Braginsky 1963, 1964): as the liquid alloy (iron plus an admixture of lighter elements) of which the outer core is composed, freezes onto the inner core, an excess of the lighter elements remains in the liquid phase which therefore becomes gravitationally unstable. The instability modes that are excited are strongly influenced, and indeed controlled, by Coriolis forces and by Lorentz forces associated with the ambient magnetic field, which is generally believed to be predominantly toroidal in the outer core.

Thermodynamic arguments suggest that the source of this instability is located in the 'mushy zone' at the inner core boundary (Loper & Roberts 1978, 1981; Loper 1983)—a layer of dendritic crystals which forms in order to allow the solidification process to proceed despite the low value of compositional diffusivity. This layer, estimated to have an effective thickness of the order of 1 km, behaves like a porous medium within which a density defect $\Delta\rho$, relative to the overlying liquid density ρ, is continuously generated. Experiments on model systems involving the freezing of ammonium chloride in solution (Chen & Chen 1991) indicate that the gravitational instability manifests itself through eruptions of buoyant fluid in the form of plumes emerging through 'chimneys' that are spontaneously created in the mushy zone, the lighter fluid being drawn horizontally into the chimneys from the surrounding mush. The effect of Coriolis and/or Lorentz forces on this type of instability is unknown; moreover, it must be admitted that conditions in the high-pressure liquid-metal environment near the inner core boundary (ICB) are so utterly different from those of the model experiments that the preferred patterns of convective instability may bear little resemblance to those of the experiments. What is clear, however, is that somehow the buoyant fluid of density $\rho - \Delta\rho$ that is created in the mushy zone will tend to erupt from this zone and rise through the liquid core, possibly entraining ambient liquid of density ρ in the process (Fig. 1). This picture of convection is related to that proposed by Howard (1964) for convection at high Rayleigh number (see Turner 1973, Section 7.3).

On this basis, it was suggested by Moffatt (1989, 1992) that it might be appropriate to treat the resulting convection in the outer core by considering the dynamics of individual parcels or blobs of buoyant fluid rising with vertical component of velocity w (and with a compensating downflow of an equal volume of liquid of density ρ). The net downward mass flux is manifest by the slow increase of

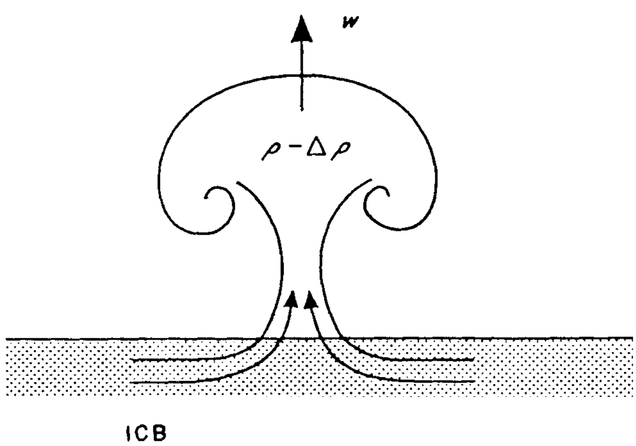

Figure 1. Schematic diagram indicating the eruption of a buoyant blob from the dendritic layer (mushy zone) on the inner core boundary (ICB).

the radius $R_1(t)$ of the inner core with density $\rho_s \approx 1.05\rho$, conservation of mass (we neglect change of volume associated with solidification of the inner core, an effect that is simply accommodated by contraction of the whole Earth) implying that

$$fw\,\Delta\rho/\rho \approx 0.05\dot{R}_1, \tag{1}$$

where f is the fraction of a spherical surface just outside the inner core occupied by rising blobs. We may reasonably assume that $f < 0.5$; the estimate $f \sim 0.1$ seems quite plausible for the purpose of numerical estimates (see below). The results appear to be qualitatively insensitive to the precise value of f provided this is not too small. Assuming a uniform rate of growth of the inner core over the lifetime of the Earth, we estimate

$$\dot{R}_1 \approx 10^{-11}\,\mathrm{m\,s^{-1}}. \tag{2}$$

A second relation between w and $\Delta\rho/\rho$ results from the assumption that the buoyancy force $\Delta\rho\mathbf{g}$ is (in order of magnitude) in balance with the Coriolis force $2\rho\mathbf{\Omega}\times\mathbf{u}$, giving the order of magnitude estimate

$$w \sim (g/\Omega)\,\Delta\rho/\rho. \tag{3}$$

Combining eqs (1) and (3), we then have the estimates

$$f^{1/2}\frac{\Delta\rho}{\rho} \sim \left(\frac{\Omega\dot{R}_1}{20g}\right)^{1/2}, \qquad f^{1/2}w \sim \left(\frac{g\dot{R}_1}{20\Omega}\right)^{1/2}, \tag{4}$$

which, with the values $\Omega = 7\times10^{-5}\,\mathrm{s^{-1}}$ and $g \sim 3\,\mathrm{m\,s^{-2}}$ (near the ICB) give

$$f^{1/2}\frac{\Delta\rho}{\rho} \sim 3\times10^{-9}, \qquad f^{1/2}w \sim 2\times10^{-4}\,\mathrm{m\,s^{-1}}. \tag{5}$$

These estimates are of course of a very preliminary character, and in particular do not take account of the possible effect of the Lorentz force on the force balance, or of the latitude dependence of Coriolis effects. Part of the aim of the present investigation is, through detailed analysis of the dynamics of a buoyant blob, to improve on the estimates (5), and to examine the general self-consistency of the 'blob model' of core dynamics.

It is noteworthy that the estimates (4) show no dependence on the length-scale a of the individual blobs. The estimate (3) does, however, require that the convective acceleration $\rho\mathbf{u}\cdot\nabla\mathbf{u}$ be negligible compared with the Coriolis acceleration $2\rho\mathbf{\Omega}\times\mathbf{u}$, i.e. the Rossby number $w/a\Omega$ must be small, or equivalently

$$a \gg w/\Omega \sim (3f^{-1/2})\,\mathrm{m} \sim 10\,\mathrm{m} \tag{6}$$

using the estimate (5) with ($f \sim 0.1$). Anticipating that the discrete plumes of fluid erupting from the mushy layer at the top of the inner core become unstable and thicken laterally (as seen in the analogue NH_4Cl experiments), the length-scale a of the blobs may be significantly larger than the radius of the chimneys from which they emanate. The chimney radius can be no smaller than the primary dendrite arm spacing (e.g. see Sarazin & Hellawell 1988), and the 'typical' spacing for planetary cores has been estimated to be several tens of metres by Esbensen (1982) by analysis of the Cape York meteorite. Consequently it is certainly reasonable to suppose that (6) is satisfied. We shall, to be specific, suppose that a is in the range 0.1–100 km in the estimates that follow.

There are then three important simplifying features in the subsequent analysis. First, the only inertial effects that need be taken into account are the Coriolis effects referred to above, the acceleration term $D\mathbf{u}/Dt = \partial\mathbf{u}/\partial t + \mathbf{u}\cdot\nabla\mathbf{u}$ in the equation of motion being negligible, by virtue of (6). Secondly, the magnetic Reynolds number

$$R_\mathrm{m} = wa/\eta \tag{7}$$

is relatively small for the range of a considered: with $\eta \approx 3\,\mathrm{m^2\,s^{-1}}$ (the usual estimate for the liquid core), we find that $R_\mathrm{m} \lesssim 7f^{-1/2} \sim 20$ when $a \lesssim 100$ km. It is therefore reasonable to suppose that the magnetic field perturbation is controlled by field diffusion and is determined instantaneously by the flow $\mathbf{u}$ across the ambient toroidal field $\mathbf{B}_0$. (The 'low R_m' approximation generally gives a good qualitative description when R_m is of order unity and even up to R_m approximately 20. Also, the structure of the solution may permit the linearization to be strictly valid for R_m exceeding unity, as was found by Ruan & Loper 1994; the range of validity may be determined *a posteriori.*) Thirdly, we shall find that viscous effects may be neglected; the formation of Taylor columns parallel to $\mathbf{\Omega}$ is suppressed by the magnetic field which (when the Lorentz force is of the same order of magnitude as the Coriolis force) ensures that the disturbance remains localized in a neighbourhood of the blob even when viscosity $\nu \to 0$.

Under these conditions, if the field $\theta(\mathbf{x}) = \Delta\rho/\rho$ is known at any instant, then both the velocity field $\mathbf{u}(\mathbf{x})$ and the magnetic field perturbation $\mathbf{b}(\mathbf{x})$ are instantaneously determined, independent of the previous history of the flow. Time dependence and non-linearity enters the problem only if we consider the evolution of the buoyancy field under the advection-diffusion equation

$$\frac{D\theta}{Dt} \equiv \frac{\partial\theta}{\partial t} + (\mathbf{u}\cdot\nabla)\theta = \kappa\nabla^2\theta \tag{8}$$

where κ is the molecular diffusivity of the compositional variation that is responsible for the density defect. If $\mathbf{u}$ is known, then eq. (8) may be used to step forward in time, with a recalculation of $\mathbf{u}$ at each time step.

In this paper, which may be regarded as an essential preliminary to any such time-dependent evolutionary study, we shall limit attention to the instantaneous problem of determining the $\mathbf{u}(\mathbf{x})$ and $\mathbf{b}(\mathbf{x})$ associated with a prescribed buoyancy field $\theta(\mathbf{x})\mathbf{g}$, where $\mathbf{g}$ is the local acceleration of gravity. In particular we shall determine the velocity at the centre of a localized spherically symmetric blob $\theta(\mathbf{x})$ of Gaussian structure

$$\theta(\mathbf{x}) = \theta_0 \exp[-|\mathbf{x}|^2/a^2], \tag{9}$$

(this is both mathematically convenient and physically natural) and we shall use this velocity to deduce the path of such a blob from the ICB to the CMB. We shall also consider some qualitative features of the full velocity field $\mathbf{u}(\mathbf{x})$, and estimate the possible effects of turbulent mixing of the blob with its surroundings. Finally, we discuss the prospects for constructing a theory of the geodynamo based on this type of blob model.

Some aspects of the dynamics of *plumes* (as opposed to *blobs*) under the influence of Coriolis and Lorentz forces have been considered in a parallel paper (Loper & Moffatt 1993).

2 GOVERNING EQUATIONS

The equations governing the coupled evolution of the velocity field $\mathbf{u}(\mathbf{x}, t)$, magnetic field $\mathbf{B}(\mathbf{x}, t)$ and buoyancy field $\theta(\mathbf{x}, t)\mathbf{g}$, in the Boussinesq approximation, are

$$\frac{D\mathbf{u}}{Dt} + 2\mathbf{\Omega}\times\mathbf{u} = -\nabla P + \frac{1}{\mu_0\rho}\mathbf{B}\cdot\nabla\mathbf{B} - \theta\mathbf{g} + \nu\nabla^2\mathbf{u}, \tag{10}$$

$$\frac{D\mathbf{B}}{Dt} = \mathbf{B}\cdot\nabla\mathbf{u} + \eta\nabla^2\mathbf{B}, \tag{11}$$

$$\frac{D\theta}{Dt} = \kappa\nabla^2\theta, \tag{12}$$

$$\nabla\cdot\mathbf{u} = \nabla\cdot\mathbf{B} = 0, \tag{13}$$

where $D/Dt = \partial/\partial t + \mathbf{u}\cdot\nabla$, $P = \rho^{-1}(p + \mathbf{B}^2/2\mu_0)$, p is the fluid pressure, ν is the kinematic viscosity, η the magnetic diffusivity of the fluid, and $\mu_0 = 4\pi\times 10^{-7}\,\mathrm{NA}^{-2}$. The magnetic field $\mathbf{B}$ is of the form

$$\mathbf{B} = \mathbf{B}_0 + \mathbf{b}, \tag{14}$$

where $\mathbf{B}_0$ is the 'applied' field, itself a product of the dynamo mechanism, but here assumed given and locally uniform and $\mathbf{b}$ is a dynamically induced perturbation. We suppose that $\mathbf{g} = -g\mathbf{e}$ is also locally uniform (where $\mathbf{e}$ is a unit vector in the upward vertical direction).

Suppose that the typical amplitude of θ is θ_0, and that the length-scale of these variations is a. Guided by the estimate (3), we adopt as velocity scale

$$V = \theta_0 g/2\Omega \tag{15}$$

where $\Omega = |\mathbf{\Omega}|$ (see eq. 3), and we suppose that the magnetic Reynolds number

$$R_m = Va/\eta \tag{16}$$

is of order unity or less. It is then well known that

$$|\mathbf{b}| = O(R_m)B_0. \tag{17}$$

We are thus led to the following scalings: let

$$\left.\begin{matrix} \mathbf{x} = a\mathbf{x}', & t = (a/V)t', & P = (VB_0^2 a/\eta\mu_0\rho)P' \\ \theta = \theta_0\theta', & \mathbf{u} = V\mathbf{u}', & \mathbf{b} = B_0(Va/\eta)\mathbf{b}' \end{matrix}\right\}. \tag{18}$$

Substituting in eqs (10)–(13), and dropping the dashes, we obtain the dimensionless equations

$$N^2\left[Ro\frac{D\mathbf{u}}{Dt} + \hat{\mathbf{\Omega}}\times\mathbf{u}\right] = -\nabla P + (\hat{\mathbf{B}}_0\cdot\nabla)\mathbf{b} + R_m\mathbf{b}\cdot\nabla\mathbf{b} + N^2\theta\mathbf{e} + \epsilon\nabla^2\mathbf{u} \tag{10'}$$

$$R_m\left[\frac{D\mathbf{b}}{Dt} - \mathbf{b}\cdot\nabla\mathbf{u}\right] = (\hat{\mathbf{B}}_0\cdot\nabla)\mathbf{u} + \nabla^2\mathbf{b} \tag{11'}$$

$$\frac{D\theta}{Dt} = \epsilon_\kappa\nabla^2\theta \tag{12'}$$

$$\nabla\cdot\mathbf{u} = \nabla\cdot\mathbf{b} = 0 \tag{13'}$$

where $\hat{\mathbf{\Omega}} = \mathbf{\Omega}/|\Omega|$, $\hat{\mathbf{B}}_0 = \mathbf{B}_0/B_0$, and where

$$N^2 = 2\Omega\mu_0\eta\rho/B_0^2 \tag{19}$$

$$Ro = V/2a\Omega \tag{20}$$

$$\epsilon = \nu\eta\mu_0\rho/B_0^2 a^2 \tag{21}$$

$$\epsilon_\kappa = \kappa/aV. \tag{22}$$

The absence of a Rayleigh number in eq. (10′) is due to the adoption of the velocity scale (15) characteristic of the balance of buoyancy and Coriolis forces. N^2 (the inverse of the Elsasser number) represents the ratio of Coriolis to Lorentz forces, and will be of order unity or somewhat less in the conditions of the liquid core. Ro is the Rossby number, of order 10^{-3} in the regime considered. The value of ϵ (the inverse square of the Hartmann number) is somewhat uncertain since the value of ν in the core is very much a matter of guesswork; if we take $\nu \sim 10^{-7}\eta$ (as for molten metals at atmospheric pressure) then we find $\epsilon \lesssim 10^{-8}$ in the core conditions; however, we will for the moment retain the viscous term in (10′) since it involves the highest derivative and is, unlike the Coriolis and magnetic terms, isotropic in structure. Finally, ϵ_κ, the inverse Peclet number, is likely to be extremely small in the core, of order 10^{-8} or even less.

For the reasons given in the introduction, we now drop the terms involving the Rossby number Ro and the magnetic Reynolds number R_m. Eqs (10′) and (11′) then take the simplified 'instantaneous', or 'quasi-static', form

$$N^2\hat{\mathbf{\Omega}}\times\mathbf{u} = -\nabla P + (\hat{\mathbf{B}}_0\cdot\nabla)\mathbf{b} + N^2\theta\mathbf{e} + \epsilon\nabla^2\mathbf{u} \tag{23}$$

$$0 = (\hat{\mathbf{B}}_0\cdot\nabla)\mathbf{u} + \nabla^2\mathbf{b} \tag{24}$$

wherein $\theta(\mathbf{x})$ will now be regarded as (instantaneously) known.

We may obtain a single equation relating $\mathbf{u}(\mathbf{x})$ and $\theta(\mathbf{x})$ by taking the curl of (23) twice, using (13′), and eliminating $\mathbf{b}$. This gives

$$-N^2(\hat{\mathbf{\Omega}}\cdot\nabla)\nabla\times\mathbf{u} = (\hat{\mathbf{B}}_0\cdot\nabla)^2\mathbf{u} - N^2\nabla\times(\mathbf{e}\times\nabla\theta) - \epsilon\nabla^4\mathbf{u}. \tag{25}$$

If we take the curl again, and eliminate $\nabla\times\mathbf{u}$ in favour of $\mathbf{u}$, we obtain the equation

$$L\mathbf{u} \equiv \left\{[\epsilon\nabla^4 - (\hat{\mathbf{B}}_0\cdot\nabla)^2]^2 + N^4(\hat{\boldsymbol{\Omega}}\cdot\nabla)^2\nabla^2\right\}\mathbf{u}$$
$$= -N^2[\epsilon\nabla^4 - (\hat{\mathbf{B}}_0\cdot\nabla)^2]\nabla\times(\mathbf{e}\times\nabla\theta) + N^4(\hat{\boldsymbol{\Omega}}\cdot\nabla)\nabla^2(\mathbf{e}\times\nabla\theta). \quad (26)$$

This linear equation may be easily solved in terms of Fourier transforms. Let

$$\hat{\theta}(\mathbf{k}) = \int \theta(\mathbf{x})e^{i\mathbf{k}\cdot\mathbf{x}}\, d^3\mathbf{x}, \quad (27)$$

with inverse

$$\theta(\mathbf{x}) = \frac{1}{(2\pi)^3}\int \hat{\theta}(\mathbf{k})e^{-i\mathbf{k}\cdot\mathbf{x}}\, d^3\mathbf{k}, \quad (28)$$

and similarly for other variables. The transform of eq. (26) is then

$$D(\mathbf{k})\hat{\mathbf{u}}(\mathbf{k}) = \{N^2[\epsilon k^4 + (\hat{\mathbf{B}}_0\cdot\mathbf{k})^2]\mathbf{k}\times(\mathbf{e}\times\mathbf{k}) + N^4(\hat{\boldsymbol{\Omega}}\cdot\mathbf{k})k^2(\mathbf{e}\times\mathbf{k})\}\,\hat{\theta}, \quad (29)$$

where

$$D(\mathbf{k}) = [\epsilon k^4 + (\hat{\mathbf{B}}_0\cdot\mathbf{k})^2]^2 + N^4k^2(\hat{\boldsymbol{\Omega}}\cdot\mathbf{k})^2. \quad (30)$$

At first sight, it looks as if the response will be dominated by contributions from the region of $\mathbf{k}$ space where $D(\mathbf{k})$ is very small, i.e. (since $\epsilon \ll 1$) from the region where $|\hat{\mathbf{B}}_0\cdot\mathbf{k}| \ll k$ and $|\hat{\boldsymbol{\Omega}}\cdot\mathbf{k}| \ll k$. This would then imply the emergence of 'pancake' structures in the plane of the vectors $\hat{\mathbf{B}}_0$, $\hat{\boldsymbol{\Omega}}$, a possibility that has recently been argued by Braginsky & Meytlis (1991). Such structures would be associated with a singular behaviour of the inverse integral for $\mathbf{u}(\mathbf{x})$ in the limit $\epsilon \to 0$ (i.e. a behaviour indicating an unbounded increase in the dimensions of the 'pancakes' in the directions of $\hat{\mathbf{B}}_0$ and $\hat{\boldsymbol{\Omega}}$). However, our detailed analysis below (Sections 3 and 5) reveals that the inverse integral actually converges when $\epsilon = 0$, provided $N \neq 0$. The structure of the velocity field is then independent of ϵ in the limit $\epsilon \to 0$, and no pancake (or columnar) structure is revealed by the exact solution when $N = O(1)$. We are thus justified in setting $\epsilon = 0$ (thereby avoiding altogether the effects of viscosity).

When $\epsilon = 0$, eq. (26) simplifies to the form

$$L\mathbf{u} = N^2(\hat{\mathbf{B}}_0\cdot\nabla)^2\nabla\times(\mathbf{e}\times\nabla\theta) + N^4(\hat{\boldsymbol{\Omega}}\cdot\nabla)\nabla^2(\mathbf{e}\times\nabla\theta), \quad (31)$$

where now

$$L = (\hat{\mathbf{B}}_0\cdot\nabla)^4 + N^4(\hat{\boldsymbol{\Omega}}\cdot\nabla)^2\nabla^2. \quad (32)$$

When $N \to 0$, the relevant limiting form of (31) is

$$(\hat{\mathbf{B}}_0\cdot\nabla)^2\mathbf{u} = N^2\nabla\times(\mathbf{e}\times\nabla\theta), \quad (33)$$

and structures become elongated in the $\hat{\mathbf{B}}_0$ direction. When $N \to \infty$, the relevant limiting form is simply

$$(\hat{\boldsymbol{\Omega}}\cdot\nabla)\mathbf{u} = \mathbf{e}\times\nabla\theta, \quad (34)$$

and in this case structures similar to Taylor columns, elongated along the direction of $\hat{\boldsymbol{\Omega}}$, must appear. The model is not strictly valid in either limit. We are, however, concerned with values of N of order unity, and in this case, as will be evident below, the disturbance remains localized in a 3-D neighbourhood of the buoyant blob.

3 SOLUTION FOR PURELY TOROIDAL FIELD

Throughout most of the liquid core, the magnetic field is believed to be predominantly toroidal due to the strong influence of differential rotation. At colatitude λ, we may therefore choose locally right-handed cartesian axes $Oxyz$, with Ox westward, Oy radially out from the rotation axis, and Oz in the direction of $\boldsymbol{\Omega}$, so that

$$\hat{\mathbf{B}}_0 = \mathbf{i}_x, \qquad \hat{\boldsymbol{\Omega}} = \mathbf{i}_z, \qquad \mathbf{e} = (0, \sin\lambda, \cos\lambda). \quad (35)$$

Then, in eq. (31), $\hat{\mathbf{B}}_0\cdot\nabla = \partial_x$, $\hat{\boldsymbol{\Omega}}\cdot\nabla = \partial_z$,

$$\nabla\times(\mathbf{e}\times\nabla\theta) = \cos\lambda(-\partial^2_{xz}\theta, -\partial^2_{yz}\theta, \partial^2_{xx}\theta + \partial^2_{yy}\theta) + \sin\lambda(-\partial^2_{xy}\theta, \partial^2_{zz}\theta + \partial^2_{xx}\theta, -\partial^2_{yz}\theta), \quad (36)$$

and

$$\partial_z(\mathbf{e}\times\nabla\theta) = \cos\lambda(-\partial^2_{yz}, \partial^2_{xz}\theta, 0) + \sin\lambda(\partial^2_{zz}\theta, 0, -\partial^2_{xz}\theta). \quad (37)$$

The solution of eq. (31) then clearly has the form

$$\mathbf{u} = (u_1, v_1, w_1)\cos\lambda + (u_2, v_2, w_2)\sin\lambda, \quad (38)$$

and if, for example, θ is an even function of x, then w_1 and v_2 will likewise be even, whereas u_1, v_1, u_2 and w_2 will all be the sum of even and odd components. The full table of such symmetries (even, odd or neither) is shown below, on the assumption that θ is an even function of all three coordinates x, y and z:

Transformation	u_1	v_1	w_1	u_2	v_2	w_2
$x\to -x$	neither	neither	even	neither	even	neither
$y\to -y$	neither	neither	even	neither	even	neither
$z\to -z$	odd	odd	even	even	even	odd
$x\to -x$, $y\to -y$	odd	odd	even	even	even	odd

Form of solution when $\epsilon = 0$

When $\epsilon = 0$, eqs (29) and (30) become

$$D(\mathbf{k})\hat{\mathbf{u}}(\mathbf{k}) = (N^2k_x^2\mathbf{k}\times(\mathbf{e}\times\mathbf{k}) + N^4k_zk^2(\mathbf{e}\times\mathbf{k}))\hat{\theta}(\mathbf{k}), \quad (39)$$

where

$$D(\mathbf{k}) = k_x^4 + N^4k^2k_z^2, \quad (40)$$

and the expression for $\mathbf{u}(\mathbf{x})$ is therefore

$$\mathbf{u}(\mathbf{x}) = \frac{1}{(2\pi)^3}\int \frac{N^2k_x^2\mathbf{k}\times(\mathbf{e}\times\mathbf{k}) + N^4k_zk^2(\mathbf{e}\times\mathbf{k})}{k_x^4 + N^4k^2k_z^2} \times \hat{\theta}(\mathbf{k})e^{-i\mathbf{k}\cdot\mathbf{x}}\, d^3\mathbf{k}. \quad (41)$$

With

$$\mathbf{e}\times\mathbf{k} = (k_z\sin\lambda - k_y\cos\lambda,\ k_x\cos\lambda,\ -k_x\sin\lambda), \quad (42)$$

and

$$\mathbf{k}\times(\mathbf{e}\times\mathbf{k}) = (-k_xk_y\sin\lambda - k_xk_z\cos\lambda,\ (k_x^2+k_z^2)\sin\lambda - k_zk_y\cos\lambda,\ (k_x^2+k_y^2)\cos\lambda - k_yk_z\sin\lambda), \quad (43)$$

we may now extract from eq. (41) formulae for the three components $[u(\mathbf{x}), v(\mathbf{x}), w(\mathbf{x})]$ of $\mathbf{u}$.

Case of a buoyant blob of spherical Gaussian structure

In order to evaluate the integral (41), we need to know the form of $\hat{\theta}(\mathbf{k})$. Choose origin $\mathbf{x}=0$ at the centre of the blob, and consider the case of a spherically symmetric Gaussian buoyancy field

$$\theta(\mathbf{x}) = e^{-|\mathbf{x}|^2} \tag{44}$$

so that

$$\hat{\theta}(\mathbf{k}) = \pi^{3/2} e^{-k^2/4}, \tag{45}$$

where $k=|\mathbf{k}|$. Let us concentrate on the velocity $\mathbf{U}=\mathbf{u}(0)$ at the centre of the blob. From eq. (41), this is given by

$$\mathbf{U} = \frac{1}{8\pi^{3/2}} \int \frac{N^2 k_x^2 \mathbf{k}\times(\mathbf{e}\times\mathbf{k}) + N^4 k_z k^2 (\mathbf{e}\times\mathbf{k})}{k_x^4 + N^4 k^2 k_z^2} e^{-k^2/4}\, d^3\mathbf{k}. \tag{46}$$

Substituting for $\mathbf{k}\times(\mathbf{e}\times\mathbf{k})$ and $\mathbf{e}\times\mathbf{k}$ from eqs (42) and (43), and retaining only those terms which are even in k_x, k_y and k_z (and do not therefore integrate to zero), we find

$$\mathbf{U} = \frac{1}{8\pi^{3/2}} \iiint_{-\infty}^{\infty} \times \frac{\{N^4 k^2 k_z^2 \sin\lambda,\ N^2 k_x^2 (k_x^2+k_z^2)\sin\lambda,\ N^2 k_x^2 (k_x^2+k_y^2)\cos\lambda\}}{k_x^4 + N^4 k^2 k_z^2} \times e^{-k^2/4}\, dk_x\, dk_y\, dk_z. \tag{47}$$

This integral may be simplified by letting $\mathbf{k}=k\boldsymbol{\kappa}$. Integrating over k using eq. 3.461(2) of Gradshteyn & Ryzhik (1980), we obtain

$$\mathbf{U} = [I_1(N)\sin\lambda,\ I_2(N)\sin\lambda,\ I_3(N)\cos\lambda], \tag{48}$$

where

$$I_1 = \frac{N^4}{4\pi}\int \frac{\kappa_z^2}{\kappa_x^4 + N^4\kappa_z^2}\, d\Omega, \tag{49}$$

$$I_2 = \frac{N^2}{4\pi}\int \frac{\kappa_x^2(\kappa_x^2+\kappa_z^2)}{\kappa_x^4 + N^4\kappa_z^2}\, d\Omega, \tag{50}$$

$$I_3 = \frac{N^2}{4\pi}\int \frac{\kappa_x^2(1-\kappa_z^2)}{\kappa_x^4 + N^4\kappa_z^2}\, d\Omega, \tag{51}$$

Ω being solid angle. These integrals may be simplified (see Appendix A) to the form

$$I_1 = 1 - \int_0^1 \frac{\mu^2}{\sqrt{\mu^4 + N^4(1-\mu^2)}}\, d\mu \tag{52}$$

$$2I_2 = I_3 = \tfrac{2}{3}N^2 \int_0^1 \frac{1+\mu^2}{\sqrt{\mu^4+N^4(1-\mu^2)}}\, d\mu. \tag{53}$$

The functions $I_1(N)$, $I_2(N)$, $I_3(N)$ are shown in Fig. 2.

The asymptotic behaviour of the integrals for large values of N is easily obtained. Eq. (52) immediately gives $I_1 \to 1$ as $N\to\infty$, while standard manipulation of the integral in eq. (53) in the limit $N\to\infty$ gives $2I_2 = I_3 = \pi/2$.

To determine the behaviour of I_1 as $N\to 0$, first rewrite eq. (52) as

$$I_1 = \int_0^1 \frac{N^4(1-\mu^2)}{\mu^4 + N^4(1-\mu^2) + \mu^2\sqrt{\mu^4+N^4(1-\mu^2)}}\, d\mu. \tag{52'}$$

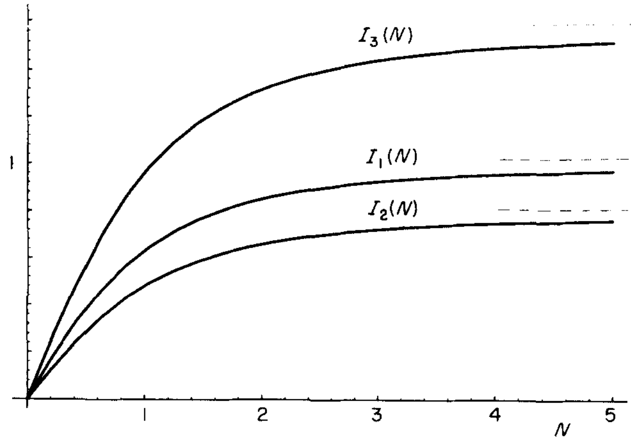

Figure 2. The functions $I_1(N)$, $I_2(N)$, $I_3(N)$ defined by the integrals (49)–(51). The asymptotic values for $N \gg 1$ are indicated by the dashed lines. Note that $I_3(N) \equiv 2I_2(N)$ and that $I_1(N) \approx \frac{2}{3}I_3(N)$ for all N.

The dominant contribution to this integral occurs for $\mu = O(N)$. Letting $\mu = N\zeta$, eq. (52′) becomes

$$I_1 = N\int_0^{1/N} \frac{1-N^2\zeta^2}{\zeta^4+1-N^2\zeta^2+\zeta^2\sqrt{\zeta^4+1-N^2\zeta^2}}\, d\zeta. \tag{54}$$

As $N\to 0$,

$$I_1 \sim N\int_0^\infty \frac{d\zeta}{\zeta^4+1+\zeta^2\sqrt{\zeta^4+1}} = \frac{N}{\sqrt{\pi}}[\Gamma(3/4)]^2 \approx 0{\cdot}847N. \tag{55}$$

Similarly

$$2I_2 = I_3 \sim \tfrac{2}{3}N\int_0^\infty \frac{d\zeta}{\sqrt{\zeta^4+1}} = \frac{N}{6\sqrt{\pi}}[\Gamma(1/4)]^2 \approx 1.236N. \tag{56}$$

The curves of Fig 2 show also that the ratio $I_1(N)/I_3(N)$ varies monotonically between 0.707 and $2/\pi \approx 0.637$ as N increases from zero to infinity. A reasonable working approximation for all N is thus given by

$$I_1(N) \approx \tfrac{4}{3}I_2(N) = \tfrac{2}{3}I_3(N). \tag{57}$$

4 TRAJECTORY OF A BUOYANT PARCEL

For simplicity, we now suppose that the velocity field $\mathbf{u}(\mathbf{x})$ within the blob is approximately uniform and therefore equal, in first approximation, to the velocity $\mathbf{U}=\mathbf{u}(0)$ determined by eq. (48). (A more detailed analysis of the structure of $\mathbf{u}(\mathbf{x})$ both inside and outside the blob is deferred to a later paper. The present analysis, in conjunction with the considerations of Sections 5 and 6, provides a reasonably simple, albeit crude, description.) This approximation finds some support from the fact that the deformation tensor $\partial u_i/\partial x_j$ is zero at $\mathbf{x}=0$ (from analysis of the symmetries of the integrand in eq. 41) and at most of order unity throughout the sphere $|\mathbf{x}|<1$ when $N=O(1)$. In this approximation, the blob retains its spherical shape, so that its velocity is given by eq. (48) at all times; we should, however, now take account of the variation of λ during the rise of the blob, and also of the possible variation of N (due

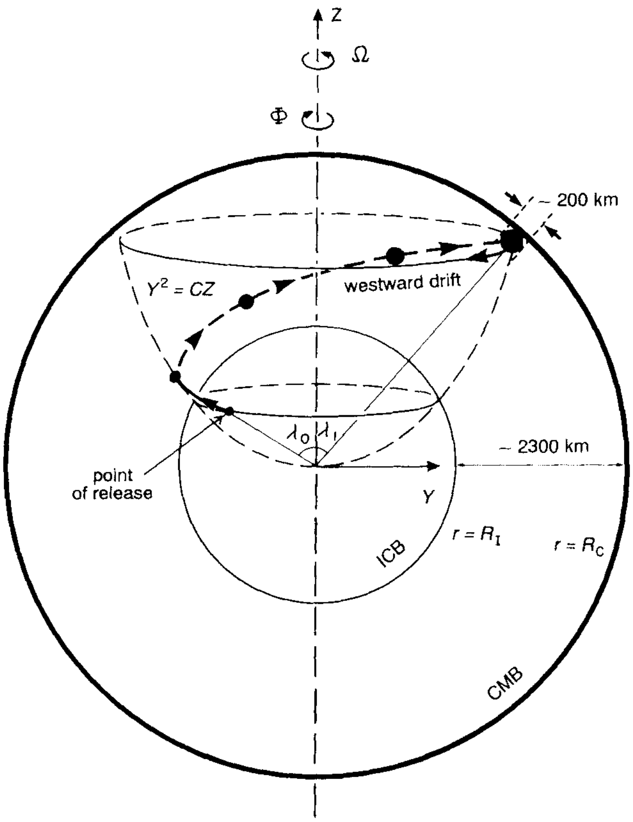

Figure 3. Notation used in Section 4. The blob follows a helical path on the paraboloid $Y^2 = CZ$, spreading by turbulent diffusion as it rises.

principally to variation of the toroidal field strength as a function of r and λ).

Let $[Y(t), Z(t)]$ be the coordinates of the centre of the blob in a meridian plane, with origin O at the centre of the Earth (Fig. 3). Then from eq. (48),

$$\left.\begin{aligned}\frac{dY}{dt} &= I_2(N)\sin\lambda = I_2(N)\frac{Y}{r}\\ \frac{dZ}{dt} &= I_3(N)\cos\lambda = I_3(N)\frac{Z}{r}\end{aligned}\right\} \tag{58}$$

where $r^2 = Y^2 + Z^2$. Hence, since $I_3(N) = 2I_2(N)$,

$$dZ/Z = 2dY/Y, \tag{59}$$

so that

$$Y^2 = CZ, \tag{60}$$

where C is a constant. This is the equation of a paraboloid of revolution about the axis OZ. The constant C is related to the colatitude λ_0 at the point of release of the blob on $r = R_I$:

$$C = \frac{Y_0^2}{\sqrt{R_I^2 - Y_0^2}} = R_I \tan\lambda_0 \sin\lambda_0. \tag{61}$$

The paraboloid intersects the CMB ($r = R_C$) at a value of Y ($= Y_1$) given by $Y_1^2 + Y_1^4/C^2 = R_C^2$, or equivalently

$$Y_1^2 = \tfrac{1}{2}R_I^2\{\tan\lambda_0 \sin\lambda_0\sqrt{\tan^2\lambda_0\sin^2\lambda_0 + 4(R_C/R_I)^2} - \tan^2\lambda_0\sin^2\lambda_0\}. \tag{62}$$

The azimuthal component of velocity on this paraboloid is given by the first component of eq. (48); note that this is positive, and that the drift is therefore in the westward direction. It may be argued in the manner of Bullard (1949) that such westward drift is an inevitable consequence of conservation of angular momentum of a rising buoyant blob; however, it is reassuring to have this heuristic argument confirmed by the above detailed calculation which takes account of the effect of the toroidal magnetic field as well as of the latitudinal dependence of Coriolis forces. (Sometimes these can conspire to promote *eastward* drift—see for example Moffatt 1978, Section 10.7; Fearn 1979). If now $\Phi(t)$ is the azimuth angle of the blob relative to its point of departure (i.e. $\Phi(0) = 0$), then

$$Y\frac{d\Phi}{dt} = I_1(N)\sin\lambda = I_1(N)\frac{Y}{r}. \tag{63}$$

Hence, using the approximate result $I_1 \approx \frac{4}{3}I_2$, we obtain

$$Y\frac{d\Phi}{dt} = \frac{4}{3}\frac{dY}{dt}, \tag{64}$$

and hence

$$\Phi = \tfrac{4}{3}\ln(Y/Y_0). \tag{65}$$

The total angle of westward drift during the rise of a blob is

$$\begin{aligned}\Phi_1 &= \tfrac{2}{3}\ln\left(\frac{Y_1^2}{Y_0^2}\right)\\ &= \tfrac{2}{3}\ln\tfrac{1}{2}\{\sec\lambda_0\sqrt{\tan^2\lambda_0\sin^2\lambda_0 + 4(R_C/R_I)^2} - \tan^2\lambda_0\}.\end{aligned} \tag{66}$$

More significantly, the velocity of westward drift of a blob when it arrives at the CMB (at $\lambda = \lambda_1$) is given by $U_1 = I_1(N)\sin\lambda_1$, where N should be based on the strength of the toroidal field within a distance of the order of the blob scale a below the CMB. The toroidal field is likely to be weaker here than at greater depth, so that the large N asymptotic estimate $I_1 \approx 1$ is likely to be a good one; the *dimensional* westward drift velocity is then

$$U_W \approx \frac{\theta_0 g}{2\Omega}\sin\lambda_1. \tag{67}$$

With the estimate $\theta_0 \sim 10^{-8}$ (from eq. 5 with $f \approx 0.1$), this gives

$$U_W \sim (0.2\sin\lambda_1)\ \mathrm{mm\,s^{-1}}, \tag{68}$$

which is of the right order of magnitude.

Similarly, the blob has a poleward component of (dimensional) velocity

$$U_P = (W\sin\lambda_1 - V\cos\lambda_1)\frac{\theta_0 g}{2\Omega} \approx \frac{\pi\theta_0 g}{8\Omega}\sin\lambda_1\cos\lambda_1 \tag{69}$$

on arrival at the CMB. Hence, the drift velocity at the CMB is tilted north of west by an angle δ where

$$\tan\delta = U_P/U_W = \frac{\pi}{4}\cos\lambda_1. \tag{70}$$

For example, at colatitude $\lambda_1 = \pi/4$, $\delta \approx 29°$, a prediction that may be testable.

The time of rise t_1 of a blob from ICB to CMB may be found from the equation

$$\frac{dZ}{dt}=I_3(N)\frac{Z}{r},\quad \text{with } r=(CZ+Z^2)^{1/2}, \tag{71}$$

provided the variation of N with depth is known. If we assume a constant value of I_3, of order unity, then eq. (71) integrates to give

$$I_3(N)t_1=[r+\tfrac{1}{2}C\ln(2r+2r\sin\lambda+C)]_{\rm ICB}^{\rm CMB}, \tag{72}$$

which may be readily converted to dimensional form. (With the estimates (5) and with $f\sim 0.1$, this rise time is of order 100 yr.)

To summarize, the blob follows a helical path on the unique paraboloid of revolution (60) passing through the point of release on the ICB; on this surface, it drifts in a westerly direction, its azimuth angle at time t relative to its point of release being given by eq. (65). On arrival at the CMB, its radial component of velocity is destroyed, and it presumably spreads out like a plume of buoyant smoke rising to the ceiling of a room. This is one mechanism whereby a relatively stable layer may be created near the CMB, a possibility proposed by Braginsky (1994). Alternatively a weakly stable mean density gradient may be established throughout the liquid core (Loper 1989) as in the analogous problem of high Rayleigh number convection already referred to in the introduction (Turner 1973, Section 73).

5 STRUCTURE OF THE VELOCITY FIELD

Substitution of the expressions (42), (43) and (45) in eq. (41) allows us to extract immediately expressions for the velocity components (u_1, v_1, w_1) and (u_2, v_2, w_2) defined by eq. (38). These may all be written in similar form, e.g.

$$u_1(\mathbf{x})=\frac{1}{8\pi^{3/2}}\int\frac{\tilde{u}_1(\mathbf{k})}{D(\mathbf{k})}e^{-k^2/4}e^{-i\mathbf{k}\cdot\mathbf{x}}\,d^3\mathbf{k}, \tag{73}$$

where $D(\mathbf{k})$ is given by eq. (40) and $\tilde{u}_1(\mathbf{k})$ is a homogeneous quartic in $\mathbf{k}$:

$$\tilde{u}_1(\mathbf{k})=-N^2k_x^3k_z-N^4k^2k_yk_z. \tag{74}$$

The similar expressions for $\tilde{v}_1(\mathbf{k})$ etc. are

$$\tilde{v}_1(\mathbf{k})=-N^2k_x^2k_yk_z+N^4k^2k_xk_z, \tag{75}$$

$$\tilde{w}_1(\mathbf{k})=N^2k_x^2(k_x^2+k_y^2), \tag{76}$$

$$\tilde{u}_2(\mathbf{k})=-N^2k_x^3k_y+N^4k^2k_z^2, \tag{77}$$

$$\tilde{v}_2(\mathbf{k})=N^2k_x^2(k_x^2+k_x^2), \tag{78}$$

$$\tilde{w}_2(\mathbf{k})=-N^2k_x^2k_yk_z-N^4k^2k_xk_z. \tag{79}$$

It is a complicated matter to investigate even the asymptotic properties for large $|\mathbf{x}|$ of integrals such as (73); we shall confine ourselves here to a demonstration that the integrals are convergent (so that the vital step of setting $\epsilon=0$ in obtaining eq. 39 is justified). It will be sufficient to consider eq. (73); all the other integrals may be treated in a similar way. Substituting (74) into eq. (73), we have

$$8\pi^{3/2}\,|u_1(\mathbf{x})|$$
$$\le\int\frac{N^2\,|k_x^3k_z|+N^4k^2\,|k_yk_z|}{D(\mathbf{k})}e^{-k^2/4}d^3\mathbf{k}$$
$$=16\sqrt{\pi}\int_0^1\int_0^{\pi/2}\frac{N^2\mu\sqrt{1-\mu^2}\,[\mu^2\sin\phi+N^2\cos\phi]}{\mu^4+N^4(1-\mu^2)\sin^2\phi}\,d\phi\,d\mu$$
$$\le 8\sqrt{\pi}\int_0^1\int_0^{\pi/2}\frac{N^2\sqrt{1-\psi}\,[\psi+N^2]}{\psi^2+N^4(1-\psi)\sin^2\phi}\,d\phi\,d\psi.$$

The integration over ϕ is standard and leaves an integral over ψ which is clearly convergent. It follows that the velocity field $u_1(\mathbf{x}, N)$ is a well-defined function of position $\mathbf{x}$ relative to the centre of the blob and of the parameter N.

The rate of release of gravitational energy due to the rise of the blob is of order $\frac{4}{3}\pi a^3(\Delta\rho)gw$, where w is the vertical component of velocity given (in dimensional form) by

$$w=\frac{g\,\Delta\rho}{2\rho\Omega}[I_3(N)\cos^2\lambda+I_2(N)\sin^2\lambda]$$
$$=\frac{g\,\Delta\rho}{2\rho\Omega}I_2(N)(1+\cos^2\lambda), \tag{80}$$

and this is exactly compensated by Joule dissipation; hence, when N is of order unity, this Joule dissipation is certainly finite and the disturbance cannot extend far from the blob itself. Detailed asymptotic analysis (which will be presented elsewhere) does in fact confirm that all components of $\mathbf{u}(\mathbf{x})$ fall off as inverse powers of $|\mathbf{x}|$ with increasing distance from the blob. (If either $N\to 0$ or $N\to\infty$, this conclusion no longer holds, and the analysis, which is based on a fluid 'of infinite extent', ceases to be valid.)

6 TURBULENT DIFFUSION OF BLOBS

The Reynolds number based on a blob scale $a\sim 10$ km, a rise velocity $w\sim 10^{-4}\,\mathrm{m\,s^{-1}}$ and a kinematic viscosity $\nu\sim 3\times 10^{-7}\,\mathrm{m^2\,s^{-1}}$ (which is just a plausible guess) is $\mathcal{R}e=wa/\nu\sim 3\times 10^6$, and turbulent entrainment of the surrounding fluid is to be expected, by the mechanism suggested by Fig. 1, which may persist throughout the rise of the blob. Actually, the turbulence may be confined to much smaller scales (of the order of $w/\Omega\sim 10$ m and less—see eq. 6) at which the non-linear term $\rho\mathbf{u}\cdot\nabla\mathbf{u}$, responsible for the cascade of energy to even smaller scales becomes important relative to the (linear) Coriolis term $2\rho\mathbf{\Omega}\times\mathbf{u}$; the Reynolds number based on this smaller scale is $\widetilde{\mathcal{R}e}=w^2/\Omega\nu\sim 3\times 10^3$, so that turbulence on scales $\lesssim w/\Omega$ will be weak (if present at all) and will have negligible influence on the spread of the blob.

In the absence of a theory of turbulence in a strongly rotating fluid permeated by a strong magnetic field, the best we can do is to make rough estimates. Suppose that turbulent diffusion does cause mixing of the blob with its surroundings so that its radius at time t is $\ell(t)$ (with $\ell(0)=a$). Let $w(t)$ be the upward velocity of the blob at time t, with $w(0)=w_0$, the velocity of release from the mushy zone on the ICB. The worst scenario (involving the most rapid mixing) involves a turbulent diffusion coefficient

$$D(T)=C_0w(t)\ell(t), \tag{81}$$

where C_0 is a constant ($C_0\approx 0.1$ in conventional turbulence contexts—see, for example, Kraichnan 1976). For the reasons indicated above, we would expect eq. (81) to be a maximal estimate.

Mass conservation implies that the density defect $\Delta\rho$ must decrease with increasing blob radius according to

$$(\Delta\rho)\ell^3 = (\Delta\rho)_0 a^3, \tag{82}$$

and the estimate (3) for w then gives

$$w(t) \sim w_0\left(\frac{r}{R_1}\right)\left(\frac{a}{\ell}\right)^3, \tag{83}$$

where we have allowed for the linear increase of g with r in the liquid core. Now the rate of spread of the blob is determined by D and ℓ alone, so that

$$\frac{d\ell}{dt} \sim \frac{D}{\ell} = C_0 w = C_0\frac{dr}{dt}, \tag{84}$$

and hence

$$\ell - a = C_0(r - R_1). \tag{85}$$

When $r = R_C$, $\ell - a \sim C_0(R_C - R_1) \sim 0.1 \times 2000\,\mathrm{km} \sim 200$ km, so that the scale of the blob is still (just) within the range for which the quasi-static approximation (23), (24) is reasonable. If, as we expect, D is in fact much less than the estimate (81), then of course the spread of the blob is correspondingly less.

Within the same approximate framework, the radial position $r(t)$ at time t is given by

$$\frac{dr}{dt} \approx \frac{w_0}{C_0^3}\left(\frac{a}{r - R_1}\right)^3\left(\frac{r}{R_1}\right) \quad (\text{for } r - R_1 \gg a). \tag{86}$$

With $\hat{r} = r/R_1$ and $k = w_0 a^3/C_0^3 R_1^4$, this integrates to give

$$kt = \tfrac{1}{6}(\hat{r} - 1)(2\hat{r}^2 - 7\hat{r} + 11) - \ln\hat{r} \tag{87}$$

(see Fig. 4). Note the strong reduction of vertical velocity due to turbulent spreading of the blob.

This simple analysis is of course quite crude, and does not take account of magnetic and Coriolis forces (other than through the geostrophic estimate (3, 83)), but its merit is that it indicates the manner of turbulent spreading and the qualitative effect that this has on rise velocity, in the simplest possible way.

Our tentative conclusion from this analysis is that, while some degree of turbulent mixing almost certainly occurs, its effects are not so strong as to undermine the assumption of coherent blob rise, upon which the main part of this paper is based. Furthermore, detailed investigation of the nature of turbulence and its diffusive properties in such an environment is desirable to corroborate this conclusion.

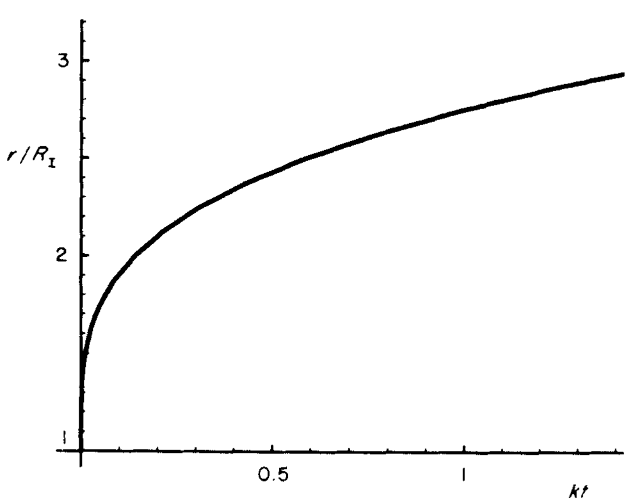

Figure 4. Radial position of a blob, subjected to turbulent diffusion, as a function of time, from equation (87).

7 DISCUSSION

The rising-blob scenario proposed in this paper provides a simple description of buoyancy-driven flow, which is quite different from the normal description based on the linear (Rayleigh-Bénard) instability of an unstably stratified layer, or annulus, of fluid. In our model, the instability is triggered in the mushy zone on the ICB, and causes the eruption of buoyant parcels, whose subsequent rise through the liquid core is an essentially non-linear phenomenon (through the non-linear advection term $\mathbf{u}\cdot\nabla\theta$ in eq. 8). By adopting certain simplifying, but plausible, assumptions concerning the scale and structure of the blobs, we have been able to bypass the non-linearity, and determine the instantaneous flow field, satisfying the magnetostrophic equation (23) and the low R_m equation for magnetic field (24), associated with a single rising blob.

Such blobs presumably erupt more or less uniformly from the mushy zone on the ICB, and follow trajectories determined by the colatitude λ_0 at the point of eruption. These trajectories are helical, with westward drift, on paraboloids of revolution with origin at the Earth's centre.

The fact that each blob satisfies the magnetostrophic equation (with zero viscosity) means that the Taylor constraint (Taylor 1963; Moffatt 1978, Chapter 12) is automatically satisfied; there is no need to invoke the effects of viscosity through Ekman or Ekman–Hartmann layers on the CMB (as has to be done, for example, in Braginsky's 'model-Z'—for a recent review see Braginsky 1991). It is an important feature of the blob scenario that the uncomfortably ill-determined viscosity of the liquid core plays no part in the theory (other than being negligible). Also, the poorly determined blob size a plays a minor role in the dynamics; all components of the velocity vector are independent of a.

Turbulence on sub-blob-scales may, however, be present, and the possible diffusive influence of such turbulence has been considered in Section 6. This will not only diffuse the compositional variation responsible for the density defect $\Delta\rho$, but will also provide an eddy viscosity which could in principle be included in a more refined analysis.

Longer term objectives must be to understand the role of such rising blobs in developing both the differential rotation and the helicity that are known to be crucial ingredients of dynamo action. The fact that rising blobs drift westward in a well-defined manner, and the associated fact that falling elements of heavier fluid drift eastward, ensures that a state of differential rotation must be established, the inner part of the liquid core rotating slightly more rapidly than the outer part. The source of helicity associated with rising blobs is more elusive, although the fact that each blob follows a helical path is presumably a relevant factor; this will be the subject of a future study.

ACKNOWLEDGMENTS

This work has been supported by NATO Collaborative Research Grant no. 901017 and by NSF via Grant no.

EAR 9116956, by the Isaac Newton Institute for Mathematical Sciences, Cambridge, under the Dynamo Theory Programme, and by the Research Institute for Mathematical Sciences, University of Kyoto, where the final version of the paper has been prepared. We thank Paul Roberts for his constructive criticisms, and in particular for his contribution of the proof that $I_3(N) = 2I_2(N)$ by the technique presented in Appendix A. The GFDI contribution number of this paper is 353.

REFERENCES

Braginsky, S.I., 1963. Structure of the *F*-layer and reasons for convection in the Earth's core, *Dokl. Akad. Nauk. SSSR*, **149**, 8–10.

Braginsky, S.I., 1964. Kinematic models of the Earth's hydromagnetic dynamo, *Geomagn. Aeron.*, **4**, 572–583.

Braginsky, S.I., 1991. Towards a realistic theory of the geodynamo, *Geophys. Astrophys. Fluid Dyn.*, **60**, 89–134.

Braginsky, S.I., 1994. MAC oscillations of the hidden ocean of the core, *J. Geomagn. Geoelect.*, in press.

Braginsky, S.I. & Meitlis, V.P., 1991. Local turbulence in the Earth's core, *Geophys. Astrophys. Fluid Dyn.*, **55**, 71–87.

Bullard, E.C., 1949. The magnetic field within the Earth, *Proc. R. Soc. Lond.*, A, **197**, 433–453.

Chen, C.F. & Chen, F. 1991. Experimental study of directional solidification of aqueous ammonium chloride solution, *J. Fluid Mech.*, **227**, 567–586.

Esbenson, K.H., 1982. Chemical and Petrological Studies in iron meteorite, *PhD thesis*, Department of Metallurgy, Technical University of Denmark.

Fearn, D., 1979. Thermally driven hydromagnetic convection in a rapidly rotating sphere, *Proc. R. Soc. Lond.*, A, **369**, 227–242.

Gradshteyn, I.S. & Ryzhik, I.M., 1980. *Table of integrals, series and products*, 4th edn, Academic Press Inc., London.

Howard, L. N., 1964. Convection at high Rayleigh number, *Proc. XIth Int. Cong. Appl. Mech.*, pp. 1109–1115, ed. Görtler, H., Springer-Verlag, Berlin.

Kraichnan, R.H., 1976. Diffusion of passive-scalar and magnetic fields by helical turbulence, *J. Fluid Mech.*, **77**, 753–768.

Loper, D.E., 1983. Structure of the inner core boundary, *Geophys. Astrophys. Fluid Dyn.*, **25**, 139–155.

Loper, D.E., 1989. Dynamo energetics and the structure of the outer core, *Geophys. Astrophys. Fluid Dyn.*, **49**, 213–219.

Loper, D.E. & Moffatt, H.K., 1993. Small-scale hydromagnetic flow in the Earth's core: Rise of a vertical buoyant plume, *Geophys. Astrophys. Fluid Dyn.*, **68**, 177–202.

Loper, D.E. & Roberts, P.H., 1978. On the motion of an iron-alloy core, containing a slurry. I. General theory, *Geophys. Astrophys. Fluid Dyn.* **9**, 289–321.

Loper, D.E. & Roberts, P.H., 1981. A study of conditions at the inner core boundary of the Earth. *Phys. Earth planet. Inter.*, **24**, 302–307.

Moffatt, H.K., 1978. *Magnetic field generation in electrically conducting fluids*, Cambridge University Press, Cambridge.

Moffatt, H.K., 1989. Liquid metal MHD and the geodynamo, in *Liquid Metal Magneto-hydrodynamics*, pp. 403–412, ed. Lielpeteris, J. & Moreau, R., Kluwer Academic Publishers, Dordrecht.

Moffatt, H.K., 1992. The Earth's magnetism: past achievements and future challenges, *IUGG Union Lectures, Vienna 1991*, pp. 1–19, Am. geophys. Un., Washington, DC.

Ruan, K. & Loper, D.E., 1994. On small-scale hydromagnetic flow in the Earth's core: Motion of a rigid cylinder parallel to its axis, *J. Geomagn. Geoelect.*, in press.

Sarazin, J.R. & Hellawell, A., 1988. Channel formation in Pb-Sn, Pb-Sb and Pb-Sn-Sb alloy ingots and comparison with the system NH_4Cl-H_2O, *Metall. Trans.*, **19A**, 1861–1871.

Taylor, J.B., 1963. The magnetohydrodynamics of a rotating fluid and the Earth's dynamo problem, *Proc. R. Soc. Lond.*, A, **274**, 274–283.

Turner, J.S., 1973. *Buoyancy Effects in Fluids*, Cambridge University Press, Cambridge.

APPENDIX A: REDUCTION OF THE INTEGRALS (49)–(51)

Introducing polar coordinates aligned with κ_x, we have

$$\kappa_x = \cos\theta = \mu, \qquad \kappa_z = \sin\theta\sin\phi \tag{A1}$$

and

$$d\Omega = d\phi\, d\mu. \tag{A2}$$

Employing the symmetries of the integrals, eqs (49)–(51) become

$$I_1 = \frac{2}{\pi}N^4\int_0^1\int_0^{\pi/2}\frac{(1-\mu^2)\sin^2\phi}{\mu^4+N^4(1-\mu^2)\sin^2\phi}\,d\phi\,d\mu \tag{A3}$$

$$I_2 = \frac{2}{\pi}N^2\int_0^1\int_0^{\pi/2}\frac{\mu^4+\mu^2(1-\mu^2)\sin^2\phi}{\mu^4+N^4(1-\mu^2)\sin^2\phi}\,d\phi\,d\mu \tag{A4}$$

$$I_3 = \frac{2}{\pi}N^2\int_0^1\int_0^{\pi/2}\frac{\mu^2-\mu^2(1-\mu^2)\sin^2\phi}{\mu^4+N^4(1-\mu^2)\sin^2\phi}\,d\phi\,d\mu. \tag{A5}$$

After integrating in ϕ with the aid of eqs 3.642(3) and 3.647 of Gradshteyn & Ryzhik (1980), the integrals may be expressed as

$$I_1 = 1 - Q_1 \tag{A6}$$

$$I_2 = \frac{1}{3N^2} + N^2Q_1 - \frac{1}{N^2}Q_2 \tag{A7}$$

$$I_3 = -\frac{1}{3N^2} + N^2Q_0 + \frac{1}{N^2}Q_2 \tag{A8}$$

where

$$Q_n = \int_0^1\frac{\mu^{2n}}{\sqrt{\mu^4+N^4(1-\mu^2)}}\,d\mu. \tag{A9}$$

The integrals Q_n may be expressed in terms of elliptic integrals of the first and second kind.

Only two of Q_0, Q_1 and Q_2 are independent. To see this, write (A9) as

$$Q_n = \int_0^1\frac{\mu^{2n}}{\sqrt{(\mu^2+a^2)(\mu^2+b^2)}}\,d\mu \tag{A10}$$

where

$$a^2+b^2 = -N^4 \quad\text{and}\quad a^2b^2 = N^4. \tag{A11}$$

Making use of eqs 3.152(1), 3.153(1) and 3.154(1) of Gradshteyn & Ryzhik (1980), we see that

$$3Q_2 - 2N^4Q_1 + N^4Q_0 = 1. \tag{A12}$$

Using this to eliminate Q_2 from eqs (A7) and (A8), the set (A6)–(A8) reduce to the form shown in eqs (52) and (53).